SCIENTIFIC PAPERS
OF THE UNIVERSITY OF PARDUBICE
Series A
Faculty of Chemical Technology
12 (2006)

FALL OF SPHERICAL PARTICLES THROUGH AN ALLEN–UHLHERR MODEL FLUID

Miloslav SIMON[a], Bedřich ŠIŠKA[a], Ludmila MACHAČOVÁ[b] and Ivan MACHAČ[a1]
[a]Department of Chemical Engineering, [b]Department of Mathematics,
The University of Pardubice, CZ–532 10 Pardubice

Received September 29, 2006

In this work, the numerical solution of Hill's variational principles is presented for the estimation of upper and lower bounds to the drag coefficient correction function necessary for the determination of terminal velocity of spherical particles falling in purely viscous fluids obeying the four-parameter Allen–Uhlherr viscosity model. The calculated data of the drag coefficient correction functions are compared with the available experimental data. In the experiments, terminal falling velocities of spheres in aqueous solutions of polyalkylene glycol Emkarox HV 45 with small addition (0.06 and 0.08 % wt) of polyacrylamide Praestol 2935 were measured. At the same time, viscosity function measurements and oscillation dynamic tests of liquids were performed using rheometer RS 150 (Haake). It was found that due to the liquid elasticity the experimental values X_{exp} of the drag coefficient correction function are beyond the calculated interval of upper and lower bounds and are higher than the upper bounds X_u. However, terminal velocities of spheres falling in fluids of the similar type as the test ones can be roughly estimated using the upper bound X_u for determination of a sphere drag coefficient.

---

[1] To whom correspondence should be addressed.

Introduction

Regarding the theoretical and practical importance of the motion of particles falling in non-Newtonian fluids, great effort has been put into investigation of the motion of spheres through non-Newtonian fluids over the last several decades. At the same time, the fluid viscosity models containing zero shear viscosity should be preferred for describing the flow of purely viscous fluids around a sphere [1,2]. Such viscosity models (especially for polymeric liquids) are, for example, the Carreau model

$$\eta = \eta_\infty + (\eta_0 - \eta_\infty)\left[1 + (\lambda\dot{\gamma})^2\right]^{\frac{m-1}{2}} \tag{1}$$

and the Allen–Uhlherr model

$$\eta = \eta_\infty + (\eta_0 - \eta_\infty)\left[1 + \lambda\dot{\gamma}\right]^{m-1} \tag{2}$$

The creeping motion of spheres through a Carreau model fluid has been solved in the work [3] using Hill's variational principles for the dimensionless viscosity parameter

$$\eta_r = \frac{\eta_0 - \eta_\infty}{\eta_0} \tag{3}$$

encompassing the interval of $1 \geq \eta_r \geq 0.5$. Here, the model parameters η_0 and η_∞ represent liquid zero shear rate and infinity shear rate viscosities, respectively.

In this work, we have formulated and solved an analogical problem for the numerical estimation of the upper and lower bounds to the drag coefficient correction function for an Allen–Uhlherr model fluid. We present the obtained dependences of the upper bound X_u and the lower bound X_l on the dimensionless time parameter Λ and the model parameter m for selected values of η_r. Some data are compared with the available experimental data X_{exp}, which were evaluated from measurements of terminal falling velocity of spherical particles moving in aqueous solutions of poly(alkylene glycol) Emkarox HV 45 with small addition of polyacrylamide Praestol 2935 under creeping flow conditions. These polymeric fluids satisfy the viscosity equation (2).

Problem Analysis

Governing Equations

Let us consider the free fall of a solid spherical particle in an unbounded purely viscous fluid whose viscosity function is approximated by the Allen–Uhlherr viscosity model. Supposing the creeping flow conditions, the problem is described by the following set of equations

continuity equation $$\nabla \cdot \vec{u} = 0 \tag{4}$$

motion equation $$\nabla p + \nabla \cdot \vec{\vec{\tau}} - \rho \vec{g} = 0 \tag{5}$$

and constitutive equation $$\vec{\vec{\tau}} = -2\eta \vec{\vec{\dot{\gamma}}} \tag{6}$$

The non-Newtonian viscosity $\eta = \eta(II)$ is the function of the second invariant of the rate of deformation tensor defined as

$$II = \sqrt{\vec{\vec{\dot{\gamma}}} : \vec{\vec{\dot{\gamma}}}} \tag{7}$$

For an Allen–Uhlherr model liquid we have

$$\eta = \eta_\infty + (\eta_0 - \eta_\infty)(1 + \sqrt{2}\lambda II)^{m-1} \tag{8}$$

In spherical coordinates (r, θ, φ), the dependent variables are the velocity components u_r, u_Θ, and the pressure p. The corresponding boundary conditions are given as

$$\text{for } r = R \quad u_r = u_\Theta = 0 \tag{9}$$
$$\text{for } r \to \infty \quad u_r = u_t \cos\theta \tag{10}$$

where R is the radius of the sphere, u_t is the terminal falling velocity.

The magnitude F_d of the drag force is gained by integration of stresses acting on the sphere surface. It can also be expressed using the drag coefficient as

$$F_D = c_D \pi R^2 (1/2) \rho u_t^2 \tag{11}$$

At the same time, the drag coefficient for the flow of the Allen–Uhlherr liquid around a sphere is given as

$$c_D = \frac{24}{Re_0} X \tag{12}$$

where the Reynolds number

$$Re_0 = \frac{2Ru_t\rho}{\eta_0} \tag{13}$$

and X is the drag coefficient correction function.

The mathematical model given by equations (4)-(13) can be approximately solved if it is replaced by an equivalent variational problem, which consists in finding a function that maximizes or minimizes a proper integral quantity (functional). Following the development of Slattery for an Ellis model fluid [4], such variational problem, based on Hill's variational principles, has also been formulated for an Allen–Uhlherr model fluid. Solving this variational problem, the upper bound X_u and the lower bound X_l to the drag coefficient correction function X can be estimated.

Upper Bound to the Drag Coefficient Correction Function

Using the first (velocity) variational principle, the following relation has been derived for the correction function X [4]

$$X = \frac{2}{3}\int_0^1\int_{-1}^1 \eta_b II_b^2 x^{-4} dy\,dx \le \frac{2}{3}\int_0^1\int_{-1}^1 E_b x^{-4} dy\,dx = \frac{2}{3}F_{ub} \tag{14}$$

Here

$$x = R/r \quad (15a) \qquad y = \cos\theta \quad (15b)$$

are the dimensionless spherical coordinates,

$$E_b = \frac{ER^2}{\eta_0 u_t^2} = (1-\eta_r)II_b^2 + \frac{\eta_r}{\Lambda^2 m(1+m)}\left[(\sqrt{2}\Lambda m II_b - 1)(\sqrt{2}\Lambda II_b + 1)^m + 1\right] \tag{16}$$

is the dimensionless function E, which is for the Allen–Uhlherr model liquid given as

$$E(II) = \int_0^{II^2} \eta(II)^2 dII^2 = \eta_\infty II^2 + \frac{\eta_0 - \eta_\infty}{\lambda^2 m(1+m)}\left[(\sqrt{2}\lambda m II - 1)(\sqrt{2}\lambda II + 1)^m + 1\right] \tag{17}$$

where

$$\eta_b = \frac{\eta}{\eta_0} \qquad (18) \qquad \Lambda = \frac{\lambda u_t}{R} \qquad (19)$$

are the dimensionless viscosity and dimensionless time parameter,

$$II_b = \frac{IIR}{u_t} = \left\{ \frac{3}{2} x^4 \left[y^2 \left(\frac{df}{dx} \right)^2 + \frac{1}{12} x^2 (1 - y^2) \left(\frac{d^2 f}{dx^2} \right)^2 \right] \right\}^{\frac{1}{2}} \qquad (20)$$

is the dimensionless second invariant of the rate of deformation tensor.

In order to express the invariant II_b, a trial velocity distribution must be specified that satisfies the continuity equation (4) and the boundary conditions (9) and (10). The equation of continuity will be fulfilled if the nonzero velocity components are written in terms of stream function

$$u_r = -\frac{1}{r^2 \sin\theta} \frac{\partial \psi}{\partial \theta} \qquad (21)$$

$$u_\theta = \frac{1}{r \sin\theta} \frac{\partial \psi}{\partial r} \qquad (22)$$

At the same time, we suppose that the stream function can be expressed by the relationship

$$\psi = -\frac{1}{2} u_t r^2 \sin^2\theta f(x) \qquad (23)$$

In our calculations, the function $f(x)$ has had the form

$$f(x) = 1 - \frac{3}{2}x + \frac{1}{2}x^3 + a(x - 2x^3 + x^5) \qquad (24)$$

in this case $\left(\frac{df}{dx} \right)_{x=1} = 0, f(1) = 0, f(0) = 1$, and $\lim_{x \to 0} x \frac{df}{dx} = 0$ so that also the boundary conditions are fulfilled. At the same time, if $a = 0$, the velocity distribution corresponds with Stokes solutions for the creeping flow of a Newtonian fluid past a sphere.

The optimum value of the parameter a in the function $f(x)$ can be determined by the minimisation of the functional F_{ub}. The estimation of the upper bound X_u to the correction function $X = X(m, \Lambda, \eta_r)$ then follows from the relation (14).

Lower Bound to the Drag Coefficient Correction Function

According to the second (stress) variational principle, the following relation is valid [4]

$$X \geq \frac{1+m}{3}\int_0^1\int_{-1}^1 E_b x^{-4} dy\,dx \geq \frac{1+m}{3} F_{lb} \tag{25}$$

The functional F_{lb} is given by the relationship

$$F_{lb} = -\int_0^1\int_{-1}^1 E_{cb} x^{-4} dy\,dx + 2B \tag{26}$$

where the function

$$E_{cb} = 2\eta_b II_b - E_b \tag{27}$$

can be determined by the solution of the equation

$$II_{\tau b} = 2\eta_b II_b \tag{28}$$

Here $II_{\tau b}$ is the dimensionless second invariant of the extra stress tensor. In order to express this invariant, a trial stress distribution that satisfies the motion equation (5) must be specified. Using the following approximations of the extra stress tensor components [4]

$$\tau_{r\theta} = B\frac{\eta_0 u_t}{R} x^4 \sin\theta \tag{29}$$

$$\tau_{\theta\theta} = \tau_{\varphi\varphi} = -\frac{1}{2}\tau_{rr} = B\frac{\eta_0 u_t}{R}(x^2 - x^4)\cos\theta \tag{30}$$

we have

$$II_{\tau b} = B\left\{2x^4\left[x^4\left(1-y^2\right) + 3\left(1-x^2\right)^2 y^2\right]\right\}^{\frac{1}{2}} \tag{31}$$

The optimum value of the parameter B can be determined by the maximization of the functional F_{lb}. The estimation of the lower bound X_l to the correction function X then follows from relation (25).

Solution Procedure

The numerical calculations of the upper bound X_u and the lower bound X_l have been performed on personal computer using tabular editor Microsoft Excel complemented by special macros compiled in Visual Basic. The calculations were performed for the varying values of quantities m, Λ, and η_r encompassing the intervals $0.2 < m \leq 1$, $0.1 \leq \Lambda \leq 2000$, and $0.5 \leq \eta_r \leq 1$.

Upper Bound

The upper bound X_u was determined by minimisation of the functional F_{ub} (Eq. (14)) using the Excel's add-on Solver. The double integral (Eq. (14)) (evaluated for each value of the parameter a) was calculated making use of extended Simpson rule. The quantity E_b, needed for the calculation of the integral, is given by Eq. (16) as a function of II_b (Eqs (20) and (24)).

Lower Bound

The lower bound X_l was determined by maximisation of the functional F_{lb} (Eq. (26)). The procedures used for the optimisation of parameter B and the double integral calculation were the same as in the case of the upper bound estimation. The necessary quantity E_{cb} is given by Eq. (27) as a function of II_b. The value of II_b was determined by the solution of the nonlinear Eq. (27).

Experimental

In our experiments, the terminal falling velocities $u_{t,w}$ of spheres in aqueous solutions of poly(alkylene glycol) Emkarox HV 45 with small addition (0.06 and 0.08 % wt) of polyacrylamide Praestol 2935 were measured [3].

The test liquids were prepared by dissolving of the corresponding amount of Praestol in 25 % aqueous solution of Emkarox HV 45. The viscosity measurements and the oscillation dynamic tests of liquids were carried out on rheometer RS 150 (Haake). The viscosity function courses were approximated by the Allen–Uhlher model (2). The resulting values of the model parameters of the

Table I Characteristics of the test liquids

Symbol	Liquid	Density ρ, kg m^{-3}	Allen–Uhlherr model parameters				
			η_0, Pa s	η_∞, Pa s	λ, s	m	η_r
L1	25 % Emkarox 0.06 % Praestol	1043	38717	0.21	1.97	0.274	0.792
L2	25 % Emkarox 0.08 % Praestol	1043	1.81	0.28	3.39	0.293	0.843

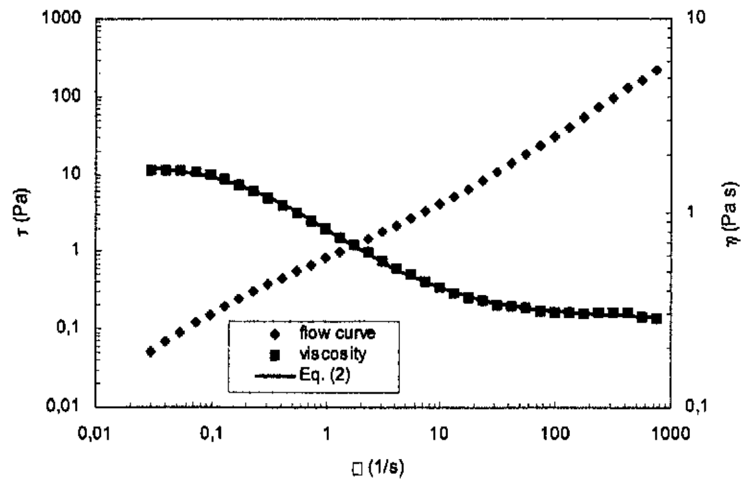

Fig. 1 Example of the flow curve and viscosity function courses for liquid L2

liquids used are given in Table I. An example of the flow and viscosity curves for the liquid L2 is shown in Fig. 1. In oscillatory tests, the comparable values of storage modulus G' and loss modulus G'' were found for both the liquids L1 and L2 as it is shown in Fig. 2. It suggests evident elasticity of the test liquids. Seven types of glass spheres were used for drop tests; their diameters and densities are given in Table II.

Wall effects were accounted for by dropping each sphere in three Perspex columns 20 mm, 40 mm, and 80 mm in diameter and about 0.8 m in length. The test section was situated nearly 0.2 m away from top and bottom ends of the tube. The range of sphere velocities encountered in these measurements was from 1.23 mm s^{-1} to 26.0 mm s^{-1}. The corresponding intervals of Reynolds number and dimensionless time parameter were $0.002 \leq Re_{\Lambda t} \leq 0.471$ and $5.6 \leq \Lambda \leq 23$, repectively.

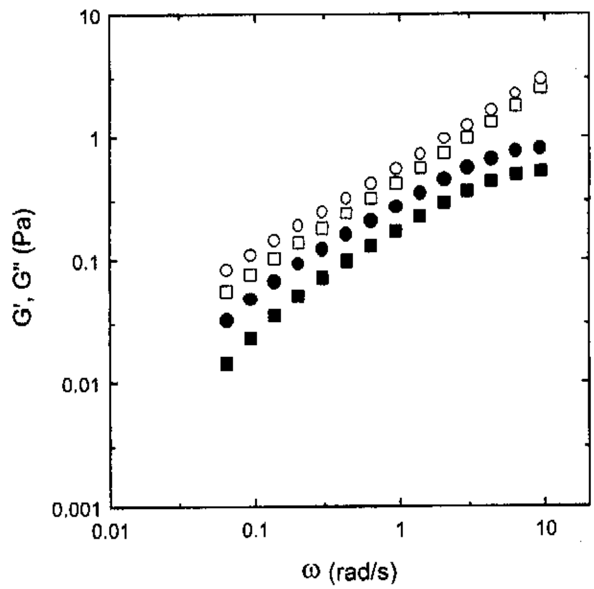

Fig. 2 Storage and loss moduli vs. angular velocity: ◇, liquid L1; O, liquid L2; empty symbols – loss modulus G''

Results and Discussion

Numerical Calculations

Examples of the results of numerical calculations of upper and lower bounds to correction function X are given in Figs 3-5 for $\eta_r = 1.0, 0.75$, and 0.5. Analogously to a Carreau model fluid, the pseudoplasticity of an Allen–Uhlher model fluid increases with the increasing value of the model parameter λ and the decreasing value of parameter m. In accordance with that, the calculated values of X_u and X_l follow the trend previously found for Carreu model fluids [3] and decrease with the increasing Λ and decreasing m for a given value of viscosity parameter η_r. At the same time, the pseudoplasticy of the above-mentioned model fluids goes down with decreasing η_r. Therefore, the smallest values of X_u and X_l for given Λ and m were obtained for $\eta_r = 1$ and their values increase with the decreasing η_r. Concerning the upper limit, $X_u \to 1$ for $\Lambda \to 0$ and any m and η_r. It corresponds with Newtonian behaviour of the fluid at this condition. On the other hand, the lower bound $X_l \to 2/(1+m)$ for $\Lambda \to 0$. Therefore, the more real estimation of the function X seems to be its upper bound X_u for low values of Λ.

Table II Characteristics of the spherical particles used

Symbol	Diameter d, mm	Density ρ_s, kg m^{-3}
S1	1.46	2464
S2	1.89	2506
S3	2.50	2516
S4	2.79	2515
S5	3.13	2463
S6	3.95	2490
S7	4.92	2514

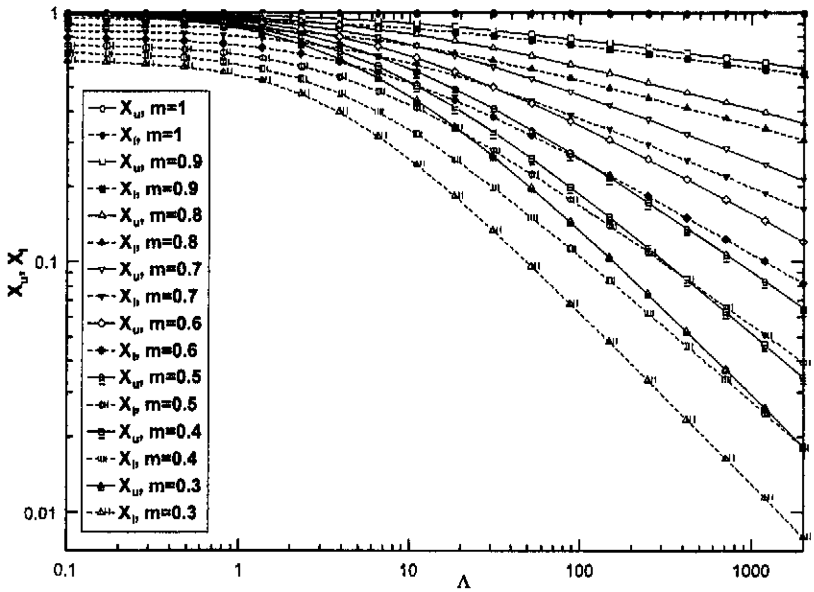

Fig. 3 Calculated values of the upper and lower bounds to correction function X as a function of dimensionless time Λ and parameter m for $\eta_r = 1$.

Comparison of Calculated and Experimental Data

The results of the numerical calculations of the function X were compared with the experimental data X_{exp} calculated from the relationship

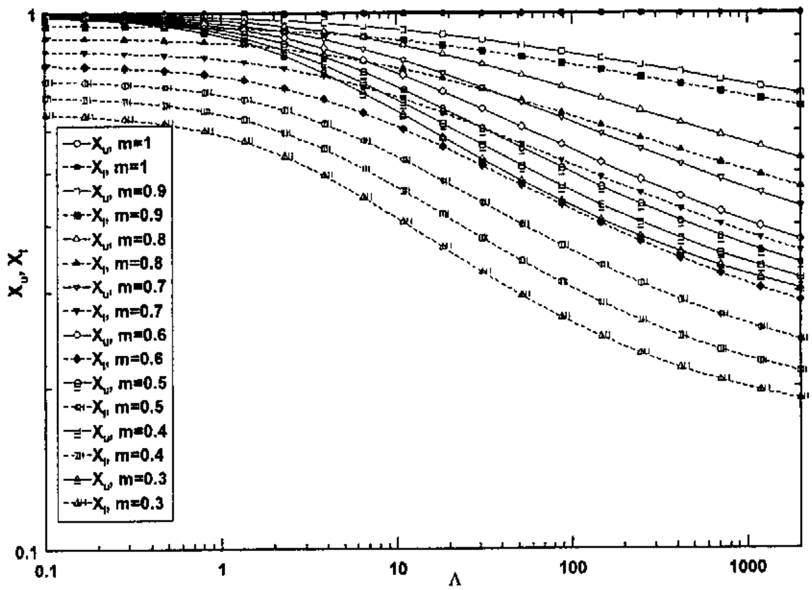

Fig. 4 Calculated values of the upper and lower bounds to correction function X as a function of dimensionless time Λ and parameter m for $\eta_r = 0.75$

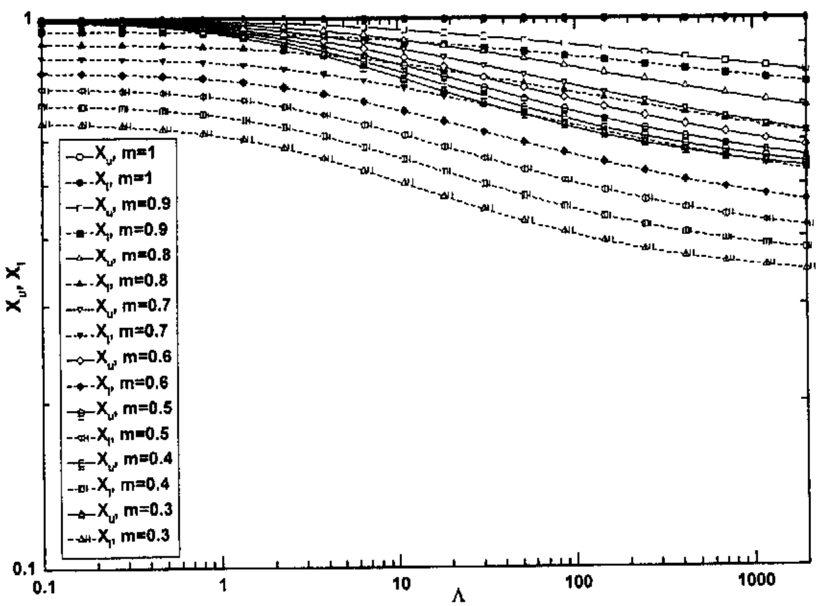

Fig. 5 Calculated values of the upper and lower bounds to correction function X as a function of dimensionless time Λ and parameter m for $\eta_r = 0.5$.

$$X_{exp} = \frac{gd^2(\rho_s - \rho)}{18\eta_0 u_{t,exp}} \tag{32}$$

which follows for

$$F_d = \frac{4}{3}\pi R^3(\rho_s - \rho)g \tag{33}$$

from Eqs (11)-(13).

The experimental values $u_{t,exp}$ of terminal falling velocity in the unbounded fluid were determined for the fall of spheres S1-S7 in both the test liquids L1 and L2 by linear extrapolation of the dependences of values $u_{t,w}$, measured in the individual test columns, on the ratio d/D to $d/D = 0$ [3] and are summarised along with the resulting values of X_{exp} in Table III. The procedure of extrapolation is illustrated in Fig. 6 where $u_{t,w}$ is plotted against d/D for spheres S1-S7 falling in the liquid L2.

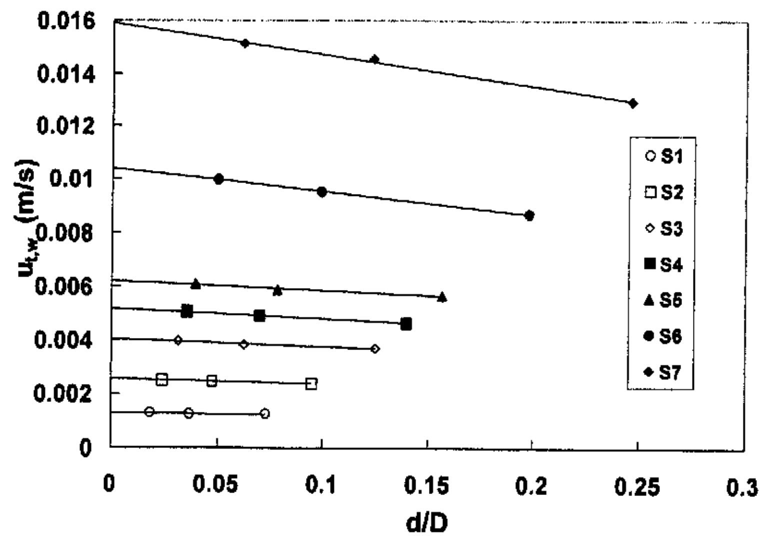

Fig. 6 Dependence of the terminal velocity of spheres S1-S7 on the diameter ratio for the liquid L2.

In Table III are also given the corresponding values of upper and lower bounds to X, which were calculated for the values of η_r, m, and Λ characterising the test liquids L1 and L2. In accordance with the previous results for Carreau mo-

Table III Comparison of the experimental values X_{exp} of drag coefficient correction function with calculated data of its upper bound X_u and lower *bound* X_l

Sphere	Liquid L1, η_r = 0.79, m = 0.274					
	$u_{t,exp}$ mm s^{-1}	Λ_{exp}	X_{exp}	X_u	X_l	δ_u %
S1	2.08	5.6	0.740	0.695	0.432	–6.2
S2	3.86	8.0	0.689	0.644	0.398	–6.5
S3	6.48	10	0.720	0.613	0.376	–14.9
S4	8.33	12	0.699	0.595	0.364	–14.8
S5	10.4	13	0.681	0.582	0.355	–14.5
S6	16.8	17	0.685	0.553	0.335	–19.2
S7	28.2	23	0.643	0.519	0.313	–19.3

Sphere	Liquid L2, η_r = 0.84, m = 0.293					
	$u_{t,exp}$ mm s^{-1}	Λ_{exp}	X_{exp}	X_u	X_l	δ_u %
S1	1.32	6.1	0.690	0.662	0.416	–4.0
S2	2.54	9.1	0.618	0.602	0.374	–2.7
S3	4.03	11	0.684	0.576	0.356	–15.8
S4	5.18	13	0.663	0.557	0.343	–16.1
S5	6.21	14	0.673	0.548	0.337	–18.6
S6	10.4	18	0.654	0.512	0.312	–21.6
S7	15.9	22	0.674	0.488	0.296	–27.6

del fluids [3], it was verified that, unlike the experiments with dilute aqueous solutions of only one polymer [2,5], the values of X_{exp} are beyond the calculated interval of X_u and X_l and are even higher than the upper bound X_u. At the same time, in contrast to expectation, the value of X_{exp} (proportional to the drag coefficient) does not evidently decrease with the increasing value of Λ. Therefore, the magnitude of relative deviation $\delta_u = (X_u - X_{exp})/X_{exp}$ between X_{exp} and X_u (Table III) increases with increasing Λ. The observed drag enhancement relative to a purely viscous fluid is undoubtedly caused, like in the fall of particles in Boger fluids (e.g. [6,7]), by rising elastic effects as dimensionless time Λ increases.

Regarding the prediction of terminal falling velocity of spheres in fluids of a kind the fluids tested, it was validated that the value of u_t can only approximately be determined from Eq. (32) substituting the upper bound X_u for X_{exp}. For that purpose, the dependences $X_u = X_u(\eta_r, m, \Lambda)$, calculated in this work (see Figs 3-5), were for $0.5 \le \eta_r \le 1$ (with the mean relative deviation $\bar{\delta}_u$ = 3 %) approximated by the relationship

$$X_u = \left\{\left[1 + \left(k_1 + k_2 m + k_3 m^2\right)\Lambda\right]^{k_4}\right\}^{k_5(m-1)} \tag{34}$$

where for $0 < \Lambda \leq 100$

$k_1 = 0.331$, $k_2 = 0.125$, $k_3 = -0.067$, $k_4 = 0.961$, and
$k_5 = 0.673\eta_r^2 - 0.151\eta_r + 0.151$

and for $100 < \Lambda \leq 2000$

$k_1 = 0.445$, $k_2 = -2.35$, $k_3 = 4.53$, $k_4 = 0.332$, and
$k_5 = 2.60\eta_r^2 - 1.42\eta_r + 0.572$

The measure of agreement between experimental terminal velocity data and data calculated according to Eqs (32) and (34) is shown for test liquids L1 and L2 in Fig. 7.

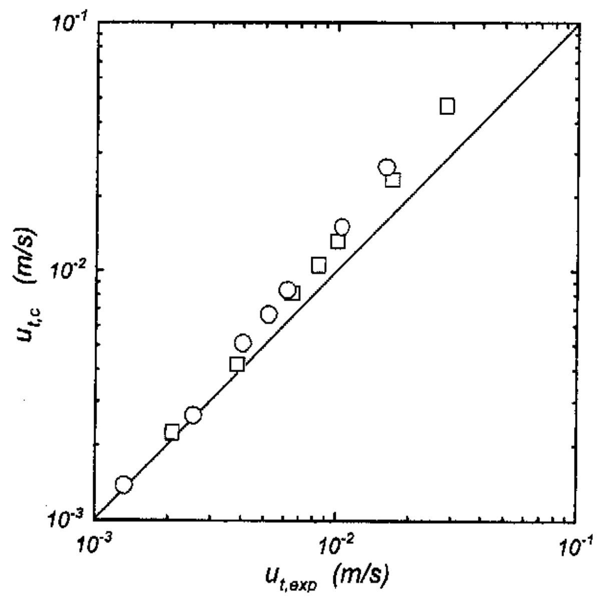

Fig. 7 Comparison of experimental terminal falling velocity data with those calculated according to Eqs (32) and (34): □, liquid L1; O, liquid L2.

The values of the relative deviations between experimental data $u_{t,exp}$ and calculated data $u_{t,c}$ range from –5 % to –66 %. At the same time, in accordance with experimental values X_{exp}, the magnitude of the deviation increases with increasing u_t due to the rising elastic effects. At the same time, the presented results of terminal falling velocity calculation are essentially the same as those obtained using the Carreau viscosity model [3].

Conclusion

Applying the Hill's variational principles, the estimations have been calculated of the upper and lower bounds to drag coefficient correction function for the fall of spherical particles in purely viscous fluids obeying the Allen–Uhlherr viscosity model. The estimations are presented by graphical dependences of the upper bound X_u and the lower bound X_l on the dimensionless time parameter Λ and the Allen–Uhlherr model parameter m for dimensionless viscosity parameter $\eta_r = 1$, 0.75, and 0.5. The calculated data of the drag coefficient correction function X are compared with the corresponding experimental data X_{exp}, which were evaluated from measurements of terminal falling velocity of spherical particles moving in pseudoplastic and elastic aqueous solutions of poly(alkylene glycol) Emkarox HV 45 with small addition of polyacrylamide Praestol 2935.

It was found that due to the liquid elasticity the obtained values of X_{exp} are beyond the calculated interval of X_u and X_l and are even higher than the upper bound X_u. In contrast to expectation, these values also do not decrease with the increasing value of Λ. In the case of the liquids tested, the elasticity effects manifest themselves more intensively than in the creeping motion of spheres through dilute viscoelastic aqueous solutions of only one polymer.

Terminal velocities of spheres falling in fluids of the type used in our measurements can only roughly be estimated using the upper bound X_u for determination of a sphere drag coefficient.

Symbols

a stream function parameter, Eq. (24)
B shear stress function parameter, Eqs (29), (30)
c_D sphere drag coefficient
d sphere diameter, m
D test column diameter, m
E function defined by Eq. (17), Pa s^{-1}
E_c function defined in dimensionless form by Eq (27), Pa s^{-1}
F functionals, Eqs (14), (26)

F_d drag force magnitude, N
g gravity acceleration, m s^{-2}
m Allen–Uhlherr model parameter
R sphere radius, m
p pressure, Pa
r radial spherical coordinate, m
Re_0 Reynolds number defined by Eq. (13)
$Re_{\Lambda t}$ $\left(= \dfrac{Re_0}{\eta_\infty/\eta_0 + \eta_r[1+\Lambda/2]^{m-1}} \right)$ Reynolds number based on the Allen–Uhlher model viscosity
x dimensionless radial spherical coordinate defined by Eq. (15a)
X drag coefficient correction function defined by Eq. (12)
y dimensionless spherical coordinate defined by Eq. (15b)
u_i velocity vector components, m s^{-1}
u_t terminal falling velocity in an unbounded fluid, m s^{-1}
$u_{t,w}$ terminal falling velocity in a test column, m s^{-1}
δ relative deviation
η non-Newtonian viscosity, Pa s
η_0 Allen–Uhlherr model parameter (zero-shear rate viscosity), Pa s
η_r dimensionless viscosity parameter defined by Eq. (3)
η_∞ Allen–Uhlherr model parameter (infinity shear rate viscosity), Pa s
θ meridian spherical coordinate
λ Allen–Uhlherr model time parameter, s
Λ dimensionless time parameter defined by Eq. (19)
ρ liquid density, kg m^{-3}
ρ_s sphere density, kg m^{-3}
$\dot{\gamma}$ shear rate, s^{-1}
$\vec{\vec{\dot{\gamma}}}$ shear rate tensor, s^{-1}
τ_{ij} extra stress tensor components, Pa
$\vec{\vec{\tau}}$ extra stress tensor, Pa
ψ stream function, Eq. (23), $m^3 s^{-1}$
II second invariant of the shear rate tensor defined by Eq. (7), s^{-1}
II_τ second invariant of the extra stress tensor given in dimensionless form by Eq. (28)

Superscripts

$\rightarrow$ vector quantity

Subscripts

b dimensionless quantity
c calculated
exp experimental value
l lower limit
r related to the radial spherical coordinate
u upper limit
θ related to the meridian spherical coordinate
φ related to the parallel spherical coordinate

References

[1] Chhabra R.P.: *Bubbles, Drops, and Particles in Non-Newtonian Fluids*, CRC Press, Boca Raton, 1993.
[2] Chhabra R.P.: Int. J. Eng. Fluid. Mech. **3**, 17 (1990).
[3] Doleček P., Bendová H., Šiška B., Machač I.: Chem. Papers **58**, 397 (2004).
[4] Slattery J.C.: *Momentum, Energy, and Mass Transfer in Continua*, McGraw-Hill, New York, 1972.
[5] Navez V., Walters K.: J. Non-Newtonian Fluid Mech. **67**, 325 (1996).
[6] Solomon M.J., Muller S.J.: J. Non-Newtonian Fluid Mech. **62**, 81 (1996).
[7] Machač I., Bendová H., Šiška B.: *Fall of a single spherical particle in Boger fluids*, 33rd International Conference of SSCHE, Tatranské Matliare, Slovakia, 2006.